Ab Initio and Density Functional Theory Studies of Proton Transfer Reactions in Multiple Hydrogen Bond Systems

Qi Zhang, Robert Bell, and Thanh N. Truong*

Department of Chemistry, University of Utah, Salt Lake City, Utah 84112

Received: July 25, 1994; In Final Form: October 18, 1994[⊗]

We have carried out both *ab initio* molecular orbital theory and density functional theory studies of mechanisms of proton transfer reactions in multiple hydrogen bond systems using formamidine and its mono-, di-, and trihydrated complexes as model systems. The highest level of *ab initio* theory, namely CCSD(T)/6-31G(d,p) at the optimized MP2 geometries, predicts the tautomerization in formamidine to have a high classical barrier of 48.8 kcal/mol. Adding one, two, or three waters to form cyclic hydrogen bond clusters stabilizes the transition state assisting proton transfer via a concerted mechanism and reduces this barrier to 21.9, 20.0, or 23.7 kcal/mol, respectively. Compared to our best *ab initio* CCSD(T)/6-31G(d,p)//MP2 results, we found that, among the local DFT JMW and VWN and nonlocal DFT B-LYP, B-P86, B3-P86, BH&H-LYP, and B3-LYP methods, only the hybrid BH&H-LYP method is capable of predicting the structure and energetic information of both the minimum energy and transition structures at a comparable accuracy with the MP2 level. We also found that using numerical atomic orbital or DFT-based Gaussian-type-orbital (GTO) basis sets yields slightly more accurate DFT results than using an HF-based GTO basis set at the 6-31G(d,p) level.

I. Introduction

This article serves two purposes. Firstly, it is designed to test the validity of the density functional method for predicting transition state properties of proton transfer reactions in multiple hydrogen bond systems, which has not previously been done. Secondly, it is a contribution toward the understanding of the mechanisms of proton transfer reactions in multiple hydrogen bond systems.

Density functional theory (DFT) has long been recognized as a better alternative tool in the study of extended metallic systems than the *ab initio* methods used in the past[1] due to the fact that it is computationally less demanding for inclusion of electron correlation. Specifically, the computational demand is formally proportional to the third power of the number of basis functions in DFT as compared to the fourth in Hartree−Fock (HF) and even higher powers in correlated HF based molecular orbital calculations. Detailed analyses[1−10] on the performance of different DFT methods had been carried out particularly for equilibrium structure properties of molecular systems, such as geometry, dipole moment, vibrational frequency, etc. The general conclusion from these studies was that DFT methods, particularly with the use of nonlocal exchange-correlation functionals, can predict accurate equilibrium structure properties. Systematic studies[11−16] on the transition state properties for other organic and inorganic reactions had also been carried out using DFT methods, and a similar conclusion was found. Recently, DFT has been used to study structures and stability of hydrogen bond complexes;[17] however, it has not been tested for studying transition state properties of reactions in multiple hydrogen bond systems such as those studied here. In this study, we have carried out in parallel both DFT and *ab initio* calculations for the transition state properties of the tautomerization of formamidine in the gas phase, as well as in mono-, di-, and trihydrated formamidine systems. We are only interested in the cyclic forms of these complexes where these water molecules are specifically located to directly assist the proton transfer process, thereby modifying the reaction path. Due to such a restriction, the modified reaction path may not be the lowest energy path for a particular cluster. The water-solvated formamidine clusters can provide some simple systems to determine the accuracy of DFT for studying proton transfer in the multiple hydrogen bond systems which are widely seen in many biological systems. By comparing DFT results with accurate *ab initio* results for these systems, we wish to establish reasonable boundary conditions and the validities of future DFT calculations on larger systems where correlated *ab initio* calculations would be unfeasible.

Proton transfer in an aqueous environment is important in virtually all biological systems. Its detailed dynamics and mechanism, particularly, the bifunctional roles of solvent, have attracted considerable research interests both theoretically and experimentally.[18−31] More specifically, solvent often assumes the traditional role of providing a heat bath and dielectric medium for the reacting system. However, solvent molecules also can act as catalysts to stabilize the transition state of the reacting system, thus, lowering the activation energy. In this paper, we examine the mechanisms of proton transfer in formamidine and in its microsolvated clusters; particularly our focus is on the role of water in assisting proton transfer processes. Note that the dimer-assisted tautomerization in formamidine had been found earlier to be more favorable than the water assisted processes;[32] it is not the key issue in this study. These reactions can be considered as basic models not only for water-catalyzed tautomerizations but also for tautomerizations in DNA bases as well as proton transfer in enzyme catalyzed reactions.[33,34] We chose to study formamidine also because it belongs to the amidine class which has been found to exhibit antibiotic, antifungal, and anesthetic activities and has been used as a basic building block in synthesizing other biologically important compounds such as purines and imidazoles.[35]

Due to its small size, many theoretical studies[32,36−41] have been carried out for the tautomerization in formamidine. The intramolecular hydrogen transfer in formamidine, a [1, 3] sigmatropic rearrangement, has a very high energetic barrier on the order of 50 kcal/mol.[32,36,38] Adding one water to assist

[⊗] Abstract published in *Advance ACS Abstracts,* December 1, 1994.

0022-3654/95/2099-0592$09.00/0

this transfer significantly reduces the barrier to the order of 20 kcal/mol.[32,36,37] The most accurate calculations[32] to date, however, include electron correlation only in the determination of the energetic properties but not in finding the transition state or equilibrium structures. Furthermore, effects on the barrier of having more than one water molecule directly assisting formamidine tautomerization had not been previously studied.

II. Methodology

For the *ab initio* MO approach, all stationary points, i.e., stable complexes and transition states, for the gas phase tautomerization and one, two, and three water assisted tautomerizations in formamidine were fully optimized at the Hartree−Fock (HF) and second-order Møller−Plesset (MP2) levels of theory by the search methods in the GAUSSIAN92/DFT program.[42] To improve the energetic predictions, particularly the barrier heights, single point MP4(SDTQ) and CCSD(T) calculations at the MP2-optimized geometries were also performed. All *ab initio* calculations were done using the 6-31G(d,p) basis set.

For DFT calculations, both local and nonlocal exchange-correlation functionals were considered. In particular, for local DFT, the Hedin−Lundqvist/Janak−Morruzi−Williams[43] local correlation functionals, denoted as JMW, and the Vosko−Wilk−Nusair[44] correlation functionals for uniform electron gas, denoted as VWN, were used. For nonlocal DFT, combinations of the Becke[45] (B), Becke's hybrid half-and-half[46] (BH&H), and Becke's three-parameter[47] (B3) gradient-corrected exchange with either the Perdew[48] (P86) or the Lee−Yang−Parr[49] (LYP) gradient-corrected correlation were used. In summary, these combinations are B-LYP, B-P86, BH&H-LYP, B3-LYP, and B3-P86. Geometries at the stationary points were optimized for each DFT method.

In this study, we have also investigated the accuracy of both the Gaussian-type-orbital (GTO) and numerical atomic orbital basis sets for DFT calculations. More specifically, for the GTO basis set, we have tested both the Hartree−Fock-based 6-31G-(d,p) and DFT-based DZVPP basis sets. DZVPP denotes (5211/411/1) contraction patterns for heavy atoms and (41/1) for hydrogen atoms.[50] For the numerical AO basis set, we employed the double numerical plus polarization atomic basis set (DNP) as implemented in the DMol program.[51]

Normal mode analyses were performed to verify that the stable complexes have all positive frequencies and, more importantly, that the transition states have only one imaginary frequency each with the corresponding eigenvector pointing toward the reactant or product. These calculations were carried out at the HF, MP2, and JMW levels of theory and the two most accurate nonlocal DFT methods for predicting barrier heights. Except for the JMW method, frequencies were calculated by analytical second derivative methods.

III. Results and Discussion

The *ab initio* and DFT results for the geometries of the stationary structures (i.e. stable complexes and transition states for the gas phase tautomerization and one, two, and three water assisted proton transfer in formamidine) are shown in Figures 1−4, respectively. The present *ab initio* results for the classical and zero-point energy corrected barrier heights, denoted respectively as $\Delta V^{\ddagger}$ and $\Delta V^{\ddagger G}$, for these reactions are listed in Table 1. The zero-point-energy-corrected barriers were determined by adding the difference between the total zero-point energies of the transition state and reactant to the classical barrier calculated at the same level of theory, except for the MP4//MP2 and CCSD(T)//MP2 results where the MP2 zero-point-energy corrections were used. DFT results for barrier heights are summarized in Tables 2 and 3.

TABLE 1: Classical Barrier Heights ($\Delta V^{\ddagger}$ kcal/mol) for Tautomerization in Formamidine and Its Microsolvated Complexes[a]

	gas phase	monohydrated	dihydrated	trihydrated
HF	61.0 (57.0)	29.3 (26.0)	30.9 (26.9)	34.8 (32.4)
MP2	47.0 (43.4)	19.5 (15.4)	17.0 (12.4)	20.5 (14.9)
MP4(SDTQ)//MP2	48.0 (44.4[b])	21.4 (17.3[b])	19.4 (14.8[b])	23.2 (17.6[b])
CCSD(T)//MP2	48.8 (45.2[b])	21.9 (17.8[b])	20.0 (15.4[b])	23.7 (18.1[b])

[a] Using the GAUSSIAN92/DFT program with the GTO 6-31G(d,p) basis set. Zero-point-energy-corrected barrier heights ($\Delta V^{\ddagger G}$, kcal/mol) are listed in parentheses. [b] MP2 zero-point energy correction is used.

TABLE 2: Comparison between *ab Initio* and Different DFT Functionals for Classical Barrier Heights ($\Delta V^{\ddagger}$, kcal/mol) of Tautomerization in Formamidine and Its Microsolvated Complexes[a]

	gas phase	monohydrated	dihydrated	trihydrated
CCSD(T)//MP2	48.8	21.9	20.0	23.7
JMW[b]	37.6	5.4	1.7	2.5
VWN[c]	36.1	6.1	2.6	2.0
B-LYP	41.8	13.6	10.8	12.7
BH&H-LYP	51.4	20.7	18.1	21.0
B3-LYP	45.6	16.2	13.4	15.7
B-P86	39.6	10.9	8.1	9.4
B3-P86	43.8	13.7	10.8	12.6

[a] Using the GAUSSIAN92/DFT program with the 6-31G(d,p) basis set unless specified. [b] Using the DMol program with the DNP basis set. [c] Using the deMon program with the DFT-based GTO DZVPP basis set.

TABLE 3: Comparison of Different Basis Sets for DFT Calculations of Classical Barrier Heights ($\Delta V^{\ddagger}$, kcal/mol) of Tautomerization in Formamidine and Its Microsolvated Complexes[a]

	gas phase	monohydrated	dihydrated	trihydrated
CCSD(T)//MP2/6-31G(d,p)	48.8	21.9	20.0	23.7
B-LYP/6-31G(d,p)	41.8	13.6	10.8	12.7
B-LYP/DNP[b]	44.4	15.3	13.0	n/a[c]
BH&H-LYP/6-31G(d,p)	51.4	20.7	18.1	21.0
BH&H-LYP/DZVPP	52.2	21.1	18.1	20.9
B3-LYP/6-31G(d,p)	45.6	16.2	13.4	15.7
B3-LYP/DZVPP	46.6	16.7	13.6	15.8
B-P86/6-31G(d,p)	39.6	10.9	8.1	9.4
B-P86/DZVPP	40.6	11.5	8.4	9.7

[a] Using the GAUSSIAN92/DFT program unless specified. [b] Using the DMol program. [c] Calculation did not converge for the transition state.

To achieve our objectives, we divide our discussion into two main parts. In part A, we focus only on the chemistry of proton transfer processes in formamidine and its water complexes. For this, we based our discussion on the results from the highest level of *ab initio* MO theory considered, namely the MP2 level for the structure determination and the CCSD(T)//MP2 level for the energetic results. In part B, we discuss the performance of different DFT functionals in predicting the transition state properties, particularly, structures, vibrational frequencies, and barrier heights, by comparing to the *ab initio* results.

A. Proton Transfers in Formamidine and Its Water Complexes. *A.1. Gas Phase and Monohydrated Formamidine Cases.* For the gas phase tautomerization process, the equilibrium formamidine and transition state structures are shown in Figure 1, parts a and b, respectively. Similarly, structures for the monohydrated formamidine system are given in Figure 2, parts a and b. Our present results are similar to those from previous calculations.[32,36−38] In particular, adding one water

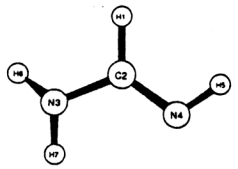

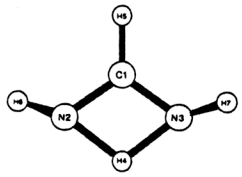

Variables	MP2	Deviation of DFT from MP2 (DFT - MP2)				
		JMW	B-P86	B-LYP	BH&H-LYP	B3-LYP
RN3C2	1.38	-0.010	0.000	0.015	-0.013	-0.002
RN4C2	1.28	-0.004	0.004	0.006	-0.021	-0.007
RH7N3	1.01	0.022	0.014	0.018	-0.007	0.003
AN3C2N4	121.5	0.48	0.46	0.62	0.89	0.62
AH7N3C2	113.4	-0.23	2.15	-0.50	1.76	1.40
DH7N3C2H1	168.3	-0.46	-0.46	-1.94	0.89	0.69

Variables	MP2	Deviation of DFT from MP2 (DFT - MP2)				
		JMW	B-P86	B-LYP	BH&H-LYP	B3-LYP
RN2C1	1.33	-0.010	0.003	0.006	-0.021	-0.007
RH4N2	1.34	0.035	0.030	0.050	-0.006	0.009
AN3C1N2	106.0	1.07	0.14	0.81	0.15	0.24
AH4N2C1	75.1	1.11	1.07	1.27	0.42	0.43
DH4N2C1N3	0.0	0.00	0.00	0.00	0.00	0.00
DH6N2C1N3	208.6	-6.02	-2.43	0.88	-4.22	-1.32

Figure 1. Optimized geometries of (a, left) the gas-phase formamidine, C_1 symmetry, (b, right) the transition state for tautomerization, C_2 symmetry. The DNP basis set was used for the JMW calculation, and the 6-31G(d,p) basis set was used for the B-P86, B-LYP, BH&H-LYP, and B3-LYP calculations. Bond lengths are in Å and angles are in deg.

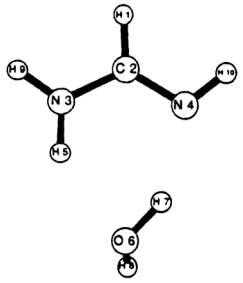

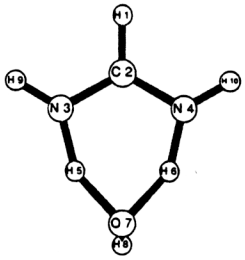

Variables	MP2	Deviation of DFT from MP2 (DFT - MP2)				
		JMW	B-P86	B-LYP	BH&H-LYP	B3-LYP
RN3C2	1.36	-0.020	0.003	0.010	-0.014	-0.004
RN4C2	1.29	0.003	0.007	0.008	-0.018	-0.004
RH5N3	1.02	0.036	0.021	0.017	-0.006	0.006
RO6H5	2.04	-0.255	-0.014	0.042	-0.020	-0.046
RH7N4	1.93	-0.284	-0.126	-0.072	-0.025	-0.048
RH7O6	0.98	0.056	0.031	0.028	-0.008	0.008
AN3C2N4	122.0	-0.15	0.21	0.44	0.69	0.25
AH5N3C2	115.3	0.53	0.63	2.59	1.39	0.62
AO6H5N3	144.7	-3.63	-3.48	-5.10	-2.05	-1.24
AH7O6H5	77.7	3.46	-0.35	-1.66	0.91	1.01
DN4C2H1N3	182.7	-1.87	-0.50	-0.25	-1.24	-0.98
DH5N3C2H1	168.7	8.51	1.43	2.21	2.75	2.07
DO6H5N3C2	10.5	-6.02	-4.76	-4.20	-2.67	-1.56
DH7O6H5N3	353.8	-3.06	4.11	4.75	0.39	-0.12
DH8O6H5N3	94.3	16.70	7.21	6.75	1.50	0.34

Variables	MP2	Deviation of DFT from MP2 (DFT - MP2)				
		JMW	B-P86	B-LYP	BH&H-LYP	B3-LYP
RN3C2	1.32	-0.003	0.008	0.011	-0.014	-0.001
RH5N3	1.21	0.026	0.010	-0.012	-0.029	0.004
RO7H5	1.30	0.006	0.031	0.089	0.026	0.012
AN4C2N3	119.0	0.43	-0.05	-0.06	0.46	0.25
AH5N3C2	107.5	0.18	0.55	1.74	0.59	0.17
AO7H5N3	151.1	-0.68	-0.42	-1.16	-0.58	-0.17
DH5N3C2N4	0.0	0.42	0.62	1.55	0.00	0.00
DO7H5N3C2	0.0	7.73	6.03	4.44	0.00	0.00
DH8O7H5N3	252.7	-11.61	-10.12	-6.50	-2.56	0.32

Figure 2. Similar to Figure 1, except for the monohydrated formamidine system: (a, left) the stable complex, C_1 symmetry, and (b, right) the transition state for tautomerization, C_s symmetry.

to form the monohydrated formamidine system as shown in Figures 2a,b significantly relaxes the gas phase formamidine transition state and consequently reduces the classical barrier from 48.8 to 21.9 kcal/mol.

A.2 Dihydrated Formamidine Case. Adding the second water can form the cyclic dihydrated formamidine complex as shown in Figure 3a,b, but the second water can also form other complexes by hydrogen bonding to the N−H or O−H bond of the monohydrated system and thus plays a spectator role to the proton transfer process.[40,41] Since we are only interested in the active role of water in assisting tautomerization, such hydrogen bond complexes are not considered in this study. For the cyclic dihydrated formamidine complex, we found that these waters forming three hydrogen bonds to formamidine further stabilize the transition state structure for tautomerization. In particular, the NCN angle is now nearly identical for both the reactant and transition state. The active NH bond is only stretched by 15%, from 1.02 to 1.17 Å at the cost of stretching two OH bonds by 23%. The classical barrier for tautomerization is lowered by another 1.9 kcal/mol from that of the monohydrated system to 20.0 kcal/mol.

A.3. Trihydrated Formamidine Case. For the same reason as indicated above, we considered only one particular trihydrated system, which has a cyclic structure where the three waters form a total of four hydrogen bonds as shown in Figure 4a,b. We found that adding three waters to form this cyclic complex destabilizes the transition state for tautomerization compared to the dihydrated case. At the transition state, the NCN angle of formamidine is bent out by 2° from the equilibrium value of 123.8°, while the active NH bonds are now stretched only by 10%. The classical barrier at the CCSD(T)//MP2 level rises back to 23.7 kcal/mol. From this result, we expect that adding even more water molecules to form larger cyclic hydrogen bond complexes with formamidine will further destabilize the transition state and consequently increase the barrier for tautomerization.

In summary, we found that water can stabilize the transition state and act as a catalyst for tautomerization in formamidine. From our analysis, we also found that the degree of stabilization of the transition state can be correlated with the extent to which the NCN angle of formamidine is bent. In particular, for the tautomerization in formamidine we found that using two water molecules to form a hydrogen bond network provides the optimal condition for stabilizing the transition state and reduces the classical barrier for tautomerization from 48.8 to 20.0 kcal/mol. The monohydrated system has only a 1.9 kcal/mol higher classical barrier.

In general, the optimal number of waters for assisting tautomerization may depend largely on the stiffness of the potential for bringing the donor and acceptor sites closer before bond breaking or forming processes start. For the formamidine tautomerization, bending the sp^2 hybrid angle at the carbon center, as our results indicate, requires substantial energy. For other types of tautomerization, such as [1, 5] hydrogen shifts,

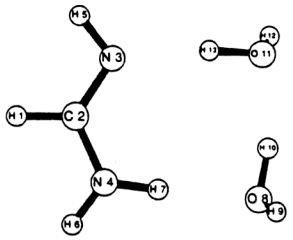

Variables	MP2	Deviation of DFT from MP2 (DFT - MP2)			
		JMW	B-P86	B-LYP	BH&H-LYP	B3-LYP
RN3C2	1.29	0.004	0.009	0.010	-0.018	-0.003
RN4C2	1.35	-0.016	0.004	0.009	-0.011	-0.002
RH7N4	1.02	0.057	0.027	0.020	-0.005	0.010
RO8H7	1.88	-0.283	-0.082	-0.017	-0.025	-0.058
RH9O8	0.96	0.021	0.015	0.022	-0.009	0.003
RH10O8	0.98	0.072	0.034	0.032	-0.008	0.011
RO11H10	1.77	-0.273	-0.099	-0.047	-0.024	-0.050
RH13N3	1.81	-0.301	-0.131	-0.074	-0.023	-0.059
RH13O11	0.99	0.088	0.042	0.037	-0.007	0.012
AN3C2N4	123.4	0.70	0.36	0.82	0.78	0.56
AH7N4C2	121.3	0.72	0.77	0.27	0.42	0.51
AO8H7N4	177.4	-4.31	-2.62	-1.68	-0.88	-1.10
AH10O8H7	94.6	0.48	0.25	-1.34	0.59	0.13
AO11H10O8	165.7	4.20	1.97	3.09	-0.69	0.84
AH13O11H10	96.3	-0.71	0.46	0.42	0.80	0.34
DH7N4C2H1	175.9	5.81	5.71	1.00	3.70	2.92
DO8H7N4C2	39.2	-6.24	-23.76	-17.51	-18.32	-23.75
DH10O8H7N4	319.0	10.58	29.03	20.53	14.10	21.65
DO11H10O8H7	14.8	-13.26	-13.39	-11.64	1.95	0.27
DH12O11H10O8	242.6	6.40	8.74	15.94	-2.41	-0.10
DH13O11H10O8	350.0	7.05	9.69	5.12	0.30	0.10

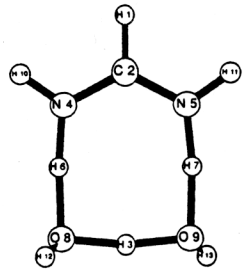

Variables	MP2	Deviation of DFT from MP2 (DFT - MP2)			
		JMW	B-P86	B-LYP	BH&H-LYP	B3-LYP
RN4C2	1.32	-0.003	0.008	0.012	-0.014	-0.000
RH6N4	1.17	0.042	0.021	0.001	-0.029	0.010
RO8H3	1.21	0.016	0.016	0.030	-0.010	0.006
RO8H6	1.34	-0.023	0.012	0.063	0.031	0.002
AN4C2N5	118.0	0.04	-0.02	0.09	0.32	0.16
AH6N4C2	122.6	-0.08	0.13	0.43	-0.07	0.00
AH6O8H3	97.8	-1.14	-0.44	-1.33	0.36	-0.07
AO8H6N4	173.2	-0.22	-0.39	-0.47	-0.36	-0.11
DH6N4C2N5	0.0	2.11	1.92	1.25	0.00	0.00
DO8H6N4C2	0.0	30.64	23.52	20.17	0.00	0.00
DH12O8H6N4	110.6	29.32	22.67	18.08	2.57	-0.34

Figure 3. Similar to Figure 1, except for the dihydrated formamidine system: (a, left) the stable complex, C_1 symmetry, and (b, right) the transition state for tautomerization, C_2 symmetry.

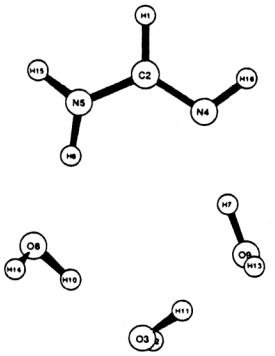

Variables	MP2	Deviation of DFT from MP2 (DFT - MP2)			
		JMW	B-P86	B-LYP	BH&H-LYP	B3-LYP
RO3C2	5.07	-0.305	-0.128	-0.063	-0.071	-0.104
RN4C2	1.29	0.004	0.009	0.008	-0.017	-0.003
RN5C2	1.35	-0.017	0.002	0.011	-0.013	-0.005
RH6N5	1.02	0.060	0.026	0.021	-0.005	0.010
RH7N4	1.79	-0.308	-0.128	-0.073	-0.021	-0.058
RO8H6	1.86	-0.270	-0.064	0.011	-0.024	-0.059
RO9H7	0.99	0.096	0.043	0.039	-0.007	0.013
RH10O8	0.98	0.072	0.034	0.033	-0.008	0.011
RH11O3	0.99	0.078	0.037	0.034	-0.008	0.011
AO3C2H1	166.8	1.38	1.98	0.64	0.78	1.79
AN4C2H1	122.6	-1.84	-0.72	-0.69	-0.66	-0.64
AN5C2H1	113.6	1.31	0.14	0.05	-0.18	-0.03
AH6N5C2	121.6	2.59	2.18	-0.09	1.35	1.87
AH7N4C2	136.7	-3.12	-0.78	0.05	-1.24	-0.66
AO8H6N5	166.4	3.76	1.44	-0.65	0.31	1.02
AO9H7N4	173.6	-1.56	1.09	0.56	0.57	0.09
AH10O8H6	112.7	0.49	-1.94	-4.66	-1.10	-2.14
AH11O3C2	52.3	-2.55	-1.68	-1.17	-0.08	-0.29
DN4C2H1O3	93.2	-4.05	2.15	-1.34	5.23	4.68
DH6N5C2H1	169.9	1.17	4.19	-3.14	5.44	5.74
DH7N4C2H1	185.4	-0.78	-2.12	-1.56	2.54	3.29
DO8H6N5C2	198.5	11.36	-3.48	-8.45	-8.00	-8.28
DO9H7N4C2	192.3	9.97	10.17	-7.40	-0.98	-7.11
DH10O8H6N5	154.1	-8.82	0.83	16.29	-2.92	-0.53
DH11O3C2N4	8.8	-4.06	-2.55	-3.10	-3.56	-5.27

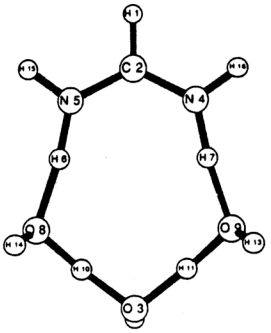

Variables	MP2	Deviation of DFT from MP2 (DFT - MP2)			
		JMW	B-P86	B-LYP	BH&H-LYP	B3-LYP
RO3C2	4.55	0.007	0.039	0.069	-0.023	-0.009
RN5C2	1.32	-0.001	0.008	0.014	-0.013	-0.000
RH6N5	1.13	0.063	0.031	0.015	-0.027	0.017
RO8H6	1.39	-0.067	-0.005	0.043	0.038	-0.010
RH10O3	1.26	-0.033	-0.004	0.017	0.017	-0.002
RH10O8	1.15	0.051	0.033	0.038	-0.028	0.012
AO3C2H1	169.4	0.27	1.26	0.41	-0.09	0.83
AN5C2H1	117.3	0.01	-0.11	-0.16	-0.32	-0.19
AH6N5C2	127.9	0.91	0.72	0.40	-0.46	0.44
AO8H6N5	171.9	0.15	0.53	-0.27	-0.23	0.20
AH10O8H6	113.4	-1.73	-0.59	-3.13	-0.31	-1.08
DN5C2H1N4	179.5	0.80	0.83	1.17	0.17	0.06
DH6N5C2H1	176.5	-0.53	1.88	-0.44	0.69	0.58
DO8H6N5C2	204.6	1.80	2.53	-3.01	-0.31	-1.50
DH10O8H6N5	141.6	0.46	-2.53	5.45	-1.29	2.16

Figure 4. Similar to Figure 1, except for the trihydrated formamidine system: (a, left) the stable complex, C_1 symmetry, and (b, right) the transition state for tautomerization, C_s symmetry.

the stress to bring the donor and acceptor closer together is distributed through the entire backbone; thus, it would require less energy, and hence a different optimal number of solvent molecules for water-assisted proton transfer would be expected.

It is interesting to point out that, from a static point of view, the present results predict the dihydrated system to have the most favorable arrangement for water assisted tautomerization in formamidine. However, from a dynamical point of view, since the transition state has more order and is tighter than the reactant, the entropy change will be negative, thus increasing the free energy of activation. Furthermore, the entropic contribution would be larger in the dihydrated system than in the monohydrated one. If such a difference in the entropy change is larger than the difference in the classical barriers of 1.9 kcal/mol, the monohydrated formamidine system could be dynamically more favorable. Thus, dynamically both the mono- and dihydrated formamidine systems are possible mechanisms for tautomerization of formamidine in aqueous solution. Dy-

namical studies of the reaction rates and kinetic isotope effects of these reactions are currently being considered using our recently developed direct *ab initio* dynamics approach.[52]

A.4. Zero-Point Energy Effects. Normal mode analyses at both the HF and MP2 levels at the stationary points confirmed the hydrogen bond complexes are equilibrium structures with all positive frequencies and the transition states all have only one imaginary frequency whose eigenvector corresponds to the motion of the reaction coordinate. Inclusion of zero-point-energy motions lowers the barriers in all cases, with the larger zero-point-energy corrections for the larger system. This result can be understood by noting the primary source of the zero-point-energy correction, namely the difference in the ground state energies of the active bonds in the reactant and transition state. For the gas phase formamidine, there is only one NH active bond, but for the mono-, di- and trihydrated systems, one, two, and three additional OH active bonds are involved in the reaction. Since these active bonds are stretched at the transition state, the zero-point-energy correction is negative and one would expect a larger correction when more active bonds are involved. Consequently, as shown in Table 1, the zero-point-energy correction at the MP2/6-31G(d,p) level lowers the classical barriers by 3.6, 4.1, 4.6, and 5.6 kcal/mol for the gas phase and mono-, di-, and trihydrated systems, respectively.

A.5 Electron Correlation Effects. Electron correlation is found to be important in determining both structures and energetic properties, particularly the barrier heights. Specifically, including electron correlation at the MP2/6-31G(d,p) level significantly shortens the hydrogen bond distances at the transition states in all hydrated systems. Moreover, correlation at the MP2 level significantly lowers the barriers by 14.0, 9.8, 12.1, and 14.3 kcal/mol for the gas phase and mono-, di-, and trihydrated formamidine systems, respectively. However, since the potential energy surface is relatively flat in the hydrogen bond degrees of freedom, the use of single-point calculations at the MP2 level using HF-optimized structures would account for most of the electron correlation contributions to the barrier heights.[32] It is interesting to note that the present results indicate electron correlation is larger at the transition states than at the equilibrium positions for the systems considered here. This is probably due to the fact that the transition states for all systems have tighter cyclic structures than the reactants. As a consequence, the lone pair electrons are more delocalized in resonance forms at the transition states, and thus electron correlation is larger.

Finally, using the fourth order perturbation theory (MP4) at the MP2 geometries raises the MP2 classical barriers by 1.0, 1.9, 2.4, and 2.7 kcal/mol, respectively, for the gas phase and mono-, di-, and trihydrated formamidine systems. More accurate single point coupled cluster calculations including single and double excitations plus noniterative triple excitation terms (CCSD(T)) raises the MP4//MP2 classical barriers in all cases by at most 0.8 kcal/mol. These data indicate that MP4//MP2 calculations are sufficient to recover most of the errors in the electron correlation at the MP2 level. In other words, second-order perturbation theory (MP2) overestimates the electron correlation contributions to the classical barrier heights for tautomerization in the formamidine system and its water complexes. This result is consistent with previous studies of formamide tautomerization in the gas phase and in its monohydrated system.[53]

B. Performance of DFT Methods for Predicting Transition State Properties. In this part, we examine the performance of different DFT methods for predicting equilibrium and transition state properties in studying proton transfer reactions

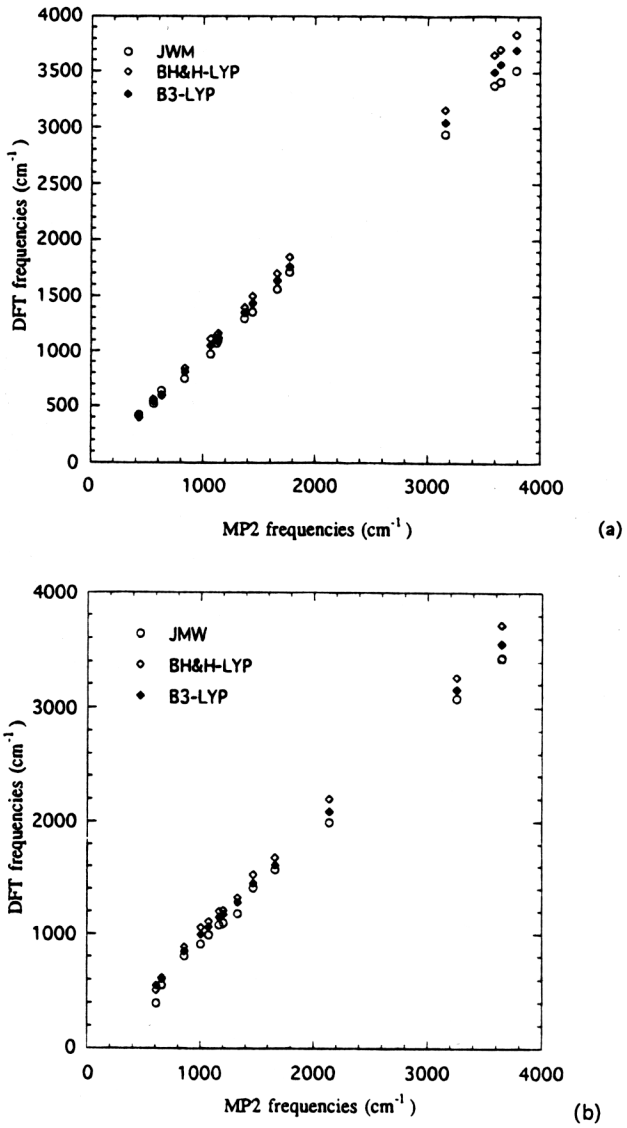

Figure 5. DFT harmonic frequencies (in cm^{-1}) versus MP2 values for (a) the formamidine gas phase and (b) the transition state for tautomerization. The DNP basis set was used for the JMW calculation, and the 6-31G(d,p) basis set was used for the BH&H-LYP and B3-LYP calculations.

in multiple hydrogen bond systems. For this discussion, we first address the differences between results from the *ab initio* and DFT methods for structures, vibrational frequencies, and barrier heights, using the same 6-31G(d,p) basis set. The basis set dependence will be discussed in a separate subsection.

B.1. Geometries. For the gas phase formamidine tautomerization where no hydrogen bond is involved, Figure 1 shows an excellent agreement geometrically between MP2 and all DFT functionals for both the stable complex structure and transition state. Both local and nonlocal DFT functionals predict structural information very similar to the MP2 results with the differences ranging from 0.001 to 0.05 Å for bond lengths and up to 6° for the angles. More specifically, BH&H-LYP and B3-LYP underestimate the bond lengths slightly.

For hydrogen bond complexes (see Figures 2–4), we found that the local DFT JMW method generally overestimates the hydrogen bond distance by 13–15% or from 0.2 to 0.3 Å. Nonlocal DFT methods improve the hydrogen bond structure significantly with the deviation from MP2 values ranging from 0.02 to 0.13 Å. This is consistent with the previous finding by Sim et al.[17] For covalent bonds, both local and nonlocal DFT functionals yield comparable results with the MP2 level.

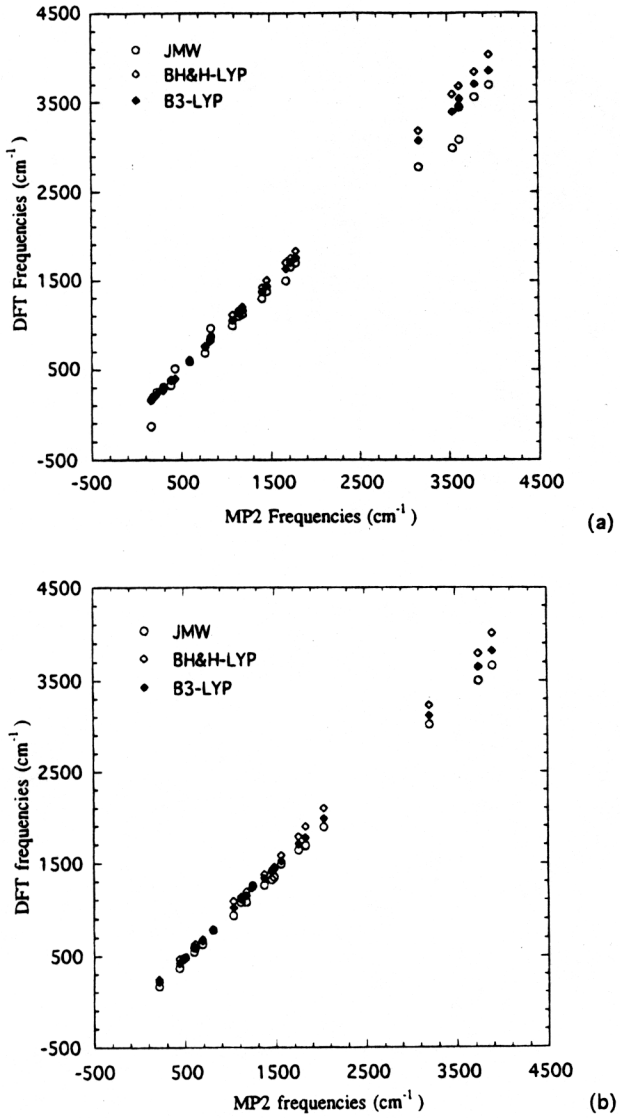

Figure 6. Similar to Figure 5, except for (a) the stable complex and (b) the transition state of the monohydrated formamidine system.

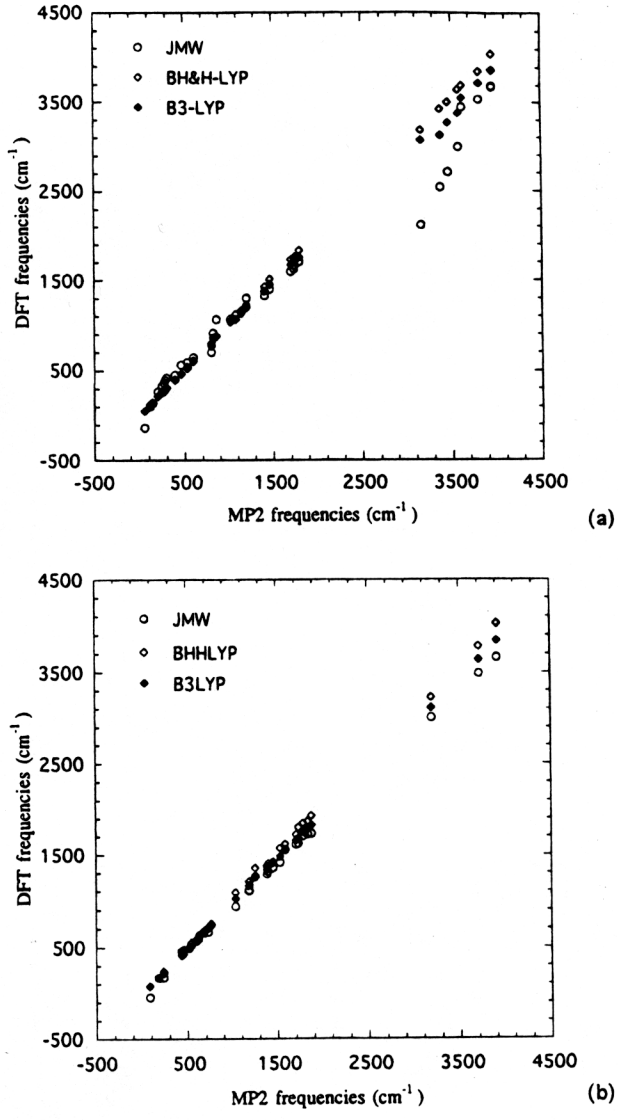

Figure 7. Similar to Figure 5, except for (a) the stable complex and (b) the transition state of the dihydrated formamidine system.

Among the nonlocal DFT functionals, the BH&H-LYP and B3-LYP methods give noticeably better agreement with the MP2 results, though the latter B3-LYP is slightly more accurate. Similar results were also obtained for the transition state structures.

B.2. Vibrational Frequencies. We have carried out normal mode analyses at the equilibrium and transition state structures using the local JMW method and the two best nonlocal methods for predicting structures, namely the BH&H-LYP and B3-LYP methods. The correlations between the DFT and MP2 frequencies are shown in Figures 5−8. The JMW method consistently yields lower frequencies compared to the MP2 results. Also for the formamidine−water complexes, it yields the wrong number of imaginary frequencies. Since these frequencies were calculated by a numerical differencing technique and the potential energy surface along the hydrogen bond modes is quite flat, the accuracy of the JMW frequency calculations is questionable. The BH&H-LYP method consistently overestimates the stretching frequencies slightly while it yields comparable accuracy with the MP2 method for lower frequency modes. The B3-LYP method gives the best agreement with MP2 frequency calculations, judging from the slopes of these correlation plots (see Figures 5−8).

B.3. Energetics. For the proton transfer processes in the gas phase, as well as through a multiple hydrogen bond network considered here, we found that the local DFT drastically underestimates the classical barriers and much more so in the hydrogen bond complexes (see Table 2). Thus, local DFT is not suitable for studying reaction mechanisms of systems involving hydrogen bonding. However, for gas phase tautomerization, it can be used to predict structures of stationary points. For the hydrogen bond complexes, nonlocal DFT methods yield significant improvements over the local DFT but still underestimate the barriers for proton transfer. In all nonlocal DFT methods considered here, only the BH&H-LYP method yields classical barriers slightly better than those of the MP2 results. In particular, the differences from the CCSD(T)//MP2 barriers for proton transfer in the gas phase and mono-, di-, and trihydrated formamidine systems, respectively, are 2.6, 1.2, 1.9, and 2.7 kcal/mol for the BH&H-LYP method as compared to 2.8, 2.4, 3.0, and 3.2 kcal/mol for the MP2 level. The B3-LYP methods yields the differences of 3.2, 5.7, 6.6, and 8.0 kcal/mol, respectively. Other nonlocal DFT methods noticeably underestimate the classical barriers. It is interesting to point out that all nonlocal DFT methods considered here yield the correct order for these barriers. In conclusion, the BH&H-LYP method gives the best prediction for barrier heights.

B.4. Basis Set Dependence. Finally, we examine the quality of different basis sets (see Table 3), namely the 6-31G(d,p), DZVPP, and DNP sets, for DFT calculations. Comparing the

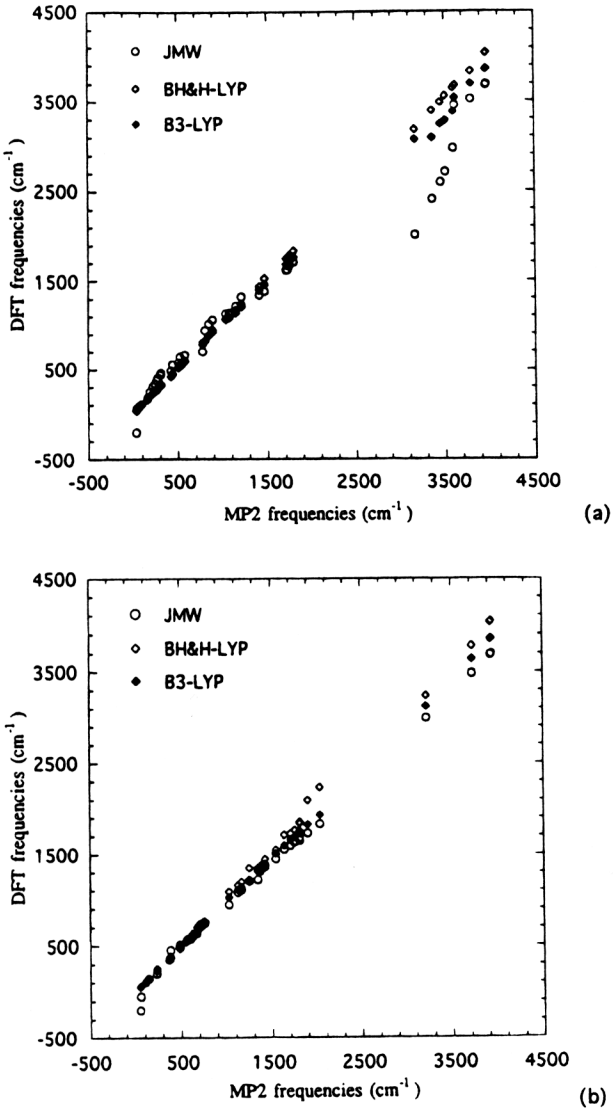

Figure 8. Similar to Figure 5, except for (a) the stable complex (b) the transition state of the trihydrated formamidine system.

B-LYP results using both the 6-31G(d,p) and DNP basis sets, we found that the DNP basis set yields a more accurate barrier heights by more than 1.5 kcal/mol. This is due to the fact that the DNP gives more accurate density distribution than the 6-31G(d,p) basis set at large distance in the region which is more important for hydrogen bonding. We also found that the DFT-based GTO DZVPP basis set improves the classical barriers in all cases by about 0.1−1.0 kcal/mol over the HF-based GTO 6-31G(d,p) basis set. Due to the size of the systems considered here, we limited our investigation at the double-ζ plus polarization, i.e. 6-31G(d,p) quality. Larger basis sets are in fact required to differentiate the effects of different types of basis sets.

In conclusion, among different DFT methods, we found that the BH&H-LYP method gives the overall best performance in predicting transition state properties, namely geometry, vibrational frequency, and barrier heights, for proton transfer processes in multiple hydrogen bond systems. The B3-LYP method yields slightly better structural and frequency information at both the equilibrium structures and transition states but noticeably underestimates the classical barrier heights.

IV. Conclusion

We have carried out *ab initio* and density functional theory studies on solvent assisted proton transfer phenomena using tautomerization in formamidine and its microsolvated complexes as model systems. We found that water can act as a catalyst for stabilizing the transition state and thus lower the barrier to tautomerization. The water molecules provide bridges that connect the donor and acceptor sites and thus relax the energy required to bring these sites closer together prior to the proton transfer process. For the 1, 3 hydrogen shift in formamidine, the high classical barrier in the gas phase is due to bending the NCN angle in the transition state. We found that the dihydrated formamidine system provides an optimal static condition and lowers the classical barrier to 20.0 kcal/mol from the gas phase value of 48.8 kcal/mol for tautomerization. However, the monohydrated system accounts for more than 90% of this barrier reduction. Thus, dynamically both mono- and dihydrated formamidine systems are possible mechanisms for water assisted tautomerization in formamidine.

We have also carried out a series of calculations to test the validity of the DFT method in the multiple hydrogen bond systems of microsolvated formamidine clusters. The local density approximation (LDA) can only provide good structure information for the gas phase system. It also significantly underestimates the classical barriers for all the systems studied here. The nonlocal exchange-correlation potentials are capable of providing excellent geometries for stationary points for all processes considered here. Comparing to our best *ab initio* CCSD(T)//MP2 results for barrier heights, we found that only the BH&H-LYP method gives overall best performance in predicting geometries, vibrational frequencies, and barrier heights for proton transfer in hydrogen bond systems. The B3-LYP method gives slightly better structural and frequency information but noticeably underestimates the barrier heights. Consequently prospects for applying the BH&H-LYP method for studying proton transfer in biological systems are encouraging.

Acknowledgment. We thank Dr. Jack Simons for helpful discussions and comments on the manuscript, Dr. Dennis Salahub for making the deMon program available, Dr. Jan Andzelm for providing the DZVPP basis set, and BIOSYM for the use of the DMol program. Q.Z. thanks the University of Utah for a faculty internship. This research was supported by the National Science Foundation (Grant CHE#9220999) and the University of Utah. T.N.T. is a recipient of a NSF Young Investigator Award.

References and Notes

(1) *Density Functional Methods in Chemistry*; Labanowski, J. K., Andzelm, J., Ed.; Springer Verlag: New York, 1991.
(2) Fitzgerald, G.; Andzelm, J. *J. Phys. Chem.* **1991**, *95*, 10531.
(3) Ziegler, T. *Pure Appl. Chem.* **1991**, *63*, 873.
(4) Andzelm, J.; Wimmer, E. *J. Chem. Phys.* **1992**, *96*, 1208.
(5) Gill, P. M. W.; Johnson, B. G.; Pople, J. A.; Frisch, M. J. *Int. J. Quantum Chem.* **1992**, *S26*, 319.
(6) Scuseria, G. E. *J. Chem. Phys.* **1992**, *97*, 7528.
(7) Dickson, R. M.; Becke, A. D. *J. Chem. Phys.* **1993**, *99*, 3898.
(8) Johnson, B. G.; Gill, P. M. W.; Pople, J. A. *J. Chem. Phys.* **1993**, *98*, 5612.
(9) Zheng, Y. C.; Almlöf, J. *Chem. Phys. Lett.* **1993**, *214*, 397.
(10) Oliphant, N.; Bartlett, R. J. *J. Chem. Phys.* **1994**, *100*, 6550.
(11) Abashkin, Y.; Russo, N. *J. Chem. Phys.* **1994**, *100*, 4477.
(12) Stanton, R. V.; Merz, K. M., Jr. *J. Chem. Phys.* **1994**, *100*, 434.
(13) Norrby, P.-O.; Kolb, H. C.; Sharpless, K. B. *Organometallics* **1994**, *13*, 344.
(14) Andzelm, J.; Sosa, C.; Eades, R. A. *J. Phys. Chem.* **1993**, *97*, 4664.
(15) Deng, L.; Ziegler, T.; Fan, L. *J. Chem. Phys.* **1993**, *99*, 3823.
(16) Fan, L.; Ziegler, T. *J. Am. Chem. Soc.* **1992**, *114*, 10890.
(17) Sim, F.; St-Amant, F. A.; Papai, I.; Salahub, D. R. *J. Am. Chem. Soc.* **1992**, *114*, 4391.
(18) Ghosh, S. K. *J. Mol. Liq.* **1993**, *57*, 75.
(19) Swinney, T. C.; Kelley, D. F. *J. Chem. Phys.* **1993**, *99*, 211.
(20) Lobaugh, J.; Voth, G. A. *Chem. Phys. Lett.* **1992**, *198*, 311.

(21) Barbara, P. F.; Walker, G. C.; Smith, T. P. *Science* **1992**, *256*, 975.
(22) Timoneda, J. J. I.; Hynes, J. T. *J. Phys. Chem.* **1991**, *95*, 431.
(23) Kim, Y. R.; Hochstrasser, R. M.; Yardley, J. T. *Chem. Phys.* **1989**, *136*, 311.
(24) Cukier, R. I.; Morillo, M. *J. Chem. Phys.* **1989**, *91*, 857.
(25) Kharakoz, D. P. *J. Acoust. Soc. Am.* **1992**, *92*, 287.
(26) Chalikian, T. V.; Kharakoz, D. P.; Sarvazyan, A. P.; Cain, C. A.; Mcgough, R. J.; Pogosova, I. V.; Gareginian, T. N. *J. Phys. Chem.* **1992**, *96*, 876.
(27) Steadman, J.; Syaga, J. A. *J. Phys. Chem.* **1991**, *95*, 326.
(28) Wiechmann, M.; Port, H.; Frey, W.; Larmer, F.; Elsasser, T. *J. Phys. Chem.* **1991**, *95*, 1918.
(29) Rumpel, H.; Limbach, H. H. *J. Am. Chem. Soc.* **1989**, *111*, 5429.
(30) Bratos, S.; Tarjus, G.; Voit, P. *J. Chem. Phys.* **1986**, *85*, 803.
(31) Chou, P.-T.; Martinez, M. L.; Cooper, W. C.; McMorrow, D.; Collins, S. T.; Kasha, M. *J. Phys. Chem.* **1992**, *96*, 5203.
(32) Nguyen, K. A.; Gordon, M. S.; Truhlar, D. G. *J. Am. Chem. Soc.* **1991**, *113*, 1596.
(33) Hilbert, F. *Avd. Phys. Org. Chem.* **1986**, *22*, 113.
(34) *Transition States of Biochemical Processes*; Gandour, R. D., Schowen, R. L., Ed.; Plenum Press: New York, 1978.
(35) Grant, R. J. In *The Chemistry of Amidines and Imidates*; Patai, S., Ed.; Wiley: New York, 1975; Chapter 6.
(36) Yamashita, K.; Kaminoyama, M.; Yamabe, T.; Fukui, K. *Theor. Chim. Acta* **1981**, *60*, 303.
(37) Yamabe, T.; Yamashita, K.; Kaminoyama, M.; Koizumi, M.; Tachibana, A.; Fukui, K. *J. Phys. Chem.* **1984**, *88*, 1459.
(38) Poirier, R. A.; Majlessi, D.; Zielinski, T. J. *J. Comput. Chem.* **1986**, *7*, 464.
(39) Nagaoka, M.; Okuno, Y.; Yamabe, T. *J. Am. Chem. Soc.* **1991**, *113*, 769.
(40) Nagaoka, M.; Okuno, Y.; Yamabe, T.; Fukui, K. *Can. J. Chem.* **1992**, *70*, 377.
(41) Nagaoka, M.; Okuno, Y.; Yamabe, T. *J. Chem. Phys.* **1992**, *97*, 8413.
(42) Frisch, M. J.; Trucks, G. W.; Head-Gordon, M.; Gill, P. M. W.; Wong, M. W.; Foresman, J. B.; Johnson, B. G.; Schlegel, H. B.; Robb, M. A.; Replogle, E. S.; Gomperts, R.; Andres, J. L.; Raghavachari, K.; Binkley, J. S.; Gonzalez, C.; Martin, R. L.; Fox, D. J.; DeFrees, D. J.; Baker, J.; Stewart, J. J. P.; Pople, J. A. *Gaussian 92*; Gaussian Inc.: Pittsburgh, PA, 1992.
(43) Hedin, L.; Lundqvist, B. I. *J. Phys. Chem.* **1971**, *4*, 2064.
(44) Vosko, S. H.; Wilk, L.; Nusair, M. *Can. J. Phys.* **1980**, *58*, 1200.
(45) Becke, A. D.; *Phys. Rev. A* **1988**, *38*, 3098.
(46) Becke, A. D. *J. Chem. Phys.* **1993**, *98*, 1372.
(47) Becke, A. D. *J. Chem. Phys.* **1993**, *98*, 5648.
(48) Perdew, J. P. *Phys. Rev. B* **1986**, *33*, 8822; erratum in *Phys. Rev. B* **1986**, *38*, 7406.
(49) Lee, C.; Yang, W.; Parr, R. G. *Phys. Rev. B* **1988**, 786.
(50) Sim, F.; Salahub, D. R.; Chin, S.; Dupuis, M. *J. Chem. Phys.* **1990**, *95*, 4317.
(51) *DMol, 2.1.0;* (Biosym Technologies: San Diego, CA 1992.
(52) Truong, T. N. *J. Chem. Phys.* **1994**, *100*, 8014.
(53) Wang, X.-C.; Nichols, J.; Feyereisen, M.; Gutowski, M.; Boatz, J.; Haymet, A. D. J.; Simons, J. *J. Phys. Chem.* **1991**, *95*, 10419.

JP9418953